Am J Cancer Res 2022;12(6):2576-2593
www.ajcr.us /ISSN:2156-6976/ajcr0141414

Original Article

Peruvoside is a novel Src inhibitor that suppresses NSCLC cell growth and motility by downregulating multiple Src-EGFR-related pathways

Yihua Lai[1,2,3,4], Hsiuhui Chang[1], Hueiwen Chen[5], Geechen Chang[6,7], Jeremy JW Chen[1,8,9]

[1]Institute of Biomedical Sciences, National Chung Hsing University, Taichung, Taiwan; [2]Rheumatic Diseases Research Center, China Medical University Hospital, Taichung, Taiwan; [3]College of Medicine, China Medical University, Taichung, Taiwan; [4]Rheumatology and Immunology Center, China Medical University Hospital, Taichung, Taiwan; [5]Graduate Institute of Toxicology, National Taiwan University College of Medicine, Taipei, Taiwan; [6]Division of Pulmonary Medicine, Department of Internal Medicine, Chung Shan Medical University Hospital, Taichung, Taiwan; [7]School of Medicine, Chung Shan Medical University, Taichung, Taiwan; [8]Biotechnology Center, National Chung Hsing University, Taichung, Taiwan; [9]Institute of Molecular Biology, National Chung Hsing University, Taichung, Taiwan

Received December 30, 2021; Accepted May 11, 2022; Epub June 15, 2022; Published June 30, 2022

Abstract: The tyrosine kinase Src plays an essential role in the progression of many cancers and is involved in several epidermal growth factor receptor (EGFR)-mediated signalling pathways. To improve the efficacy of lung cancer treatments, this study aimed to identify novel compounds that can disrupt the Src-EGFR interaction and that are less dependent on EGFR status with wild-type and mutations than other compounds. We used the Src pY419 ELISA as the platform to screen a compound library of more than 400 plant-derived active ingredients and identified peruvoside as a candidate Src-EGFR crosstalk inhibitor. The effects of peruvoside were evaluated by western blotting, cell function assays, combination Index (CI)-isobologram analyses and *in vivo* experiments. Peruvoside significantly suppressed the phosphorylation of Src, EGFR, and signal transducer and activator of transcription 3 (STAT3) in a dose- and time-dependent manner and somewhat suppressed their protein expression. Cell function assays revealed that peruvoside inhibited the proliferation, invasion, migration, and colony formation of lung cancer cells *in vitro* and tumour growth *in vivo*. Furthermore, peruvoside sensitized gefitinib-resistant tumour cells (A549, PC9/gef and H1975) to gefitinib treatment, indicating that peruvoside may exert synergistic effects when used in combination with established therapeutic agents. Our data also demonstrated that the inhibitory effects of peruvoside on lung cancer progression might be attributed to its ability to regulate Src, phosphoinositide 3-kinase (PI3K), c-Jun N-terminal kinase (JNK), Paxillin, p130cas, and EGFR. Our findings suggest that peruvoside suppresses non-small-cell lung carcinoma (NSCLC) malignancy by downregulating multiple Src-related pathways and could serve as a potential base molecule for developing new anticancer drugs and therapeutic strategies for lung cancer.

Keywords: Src, epidermal growth factor receptor, non-small-cell lung carcinoma, peruvoside, gefitinib

Introduction

Non-small-cell lung cancer (NSCLC) is one of the leading causes of cancer-related mortality worldwide. The five-year survival rate of lung cancer patients after diagnosis has plateaued at 12%-15% [1]. Mutations in oncogenic driver genes are usually the cause of dysfunction of normal cells. Most of these mutations occur in kinases related to signal transduction, such as human epidermal growth factor receptor 2 (HER2), Kirsten rat sarcoma viral oncogene homolog (KRAS), Protein kinase B (AKT), mitogen-activated protein kinase kinase (MEK), and epidermal growth factor receptor (EGFR); these mutations result in constitutive activation and overexpression (thereby inducing abnormal cancer cell growth and metastasis), which leads to poor prognoses and poor treatment responses [2, 3]. Therefore, targeting these molecules of HER2, KRAS, AKT, MEK, and EGFR to inhibit tumour growth is essential to improve the prognosis of NSCLC patients and increase the treatment efficiency for this disease [4].

In recent years, targeted therapies have been developed to treat NSCLC patients with certain driver mutations. EGFR tyrosine kinase inhibitors (TKIs), such as gefitinib and erlotinib, function by competing for the ATP-binding site and have been used in clinical treatment [5]. The sensitivity of these drugs is related to the position of the mutation on the tyrosine kinase domain of EGFR. For example, the lack of exon 19 and the L858R mutation in exon 21 can increase drug sensitivity [6]. Conversely, the EGFR T790M mutation can lead to TKI resistance and is positively associated with lung cancer recurrence [7]. In addition, previous research has indicated that primary resistance of NSCLCs to EGFR TKIs is mostly associated with wild-type EGFR [8]. Drug resistance is a crucial issue in cancer treatment; therefore, the development of new therapeutic strategies or targeted drugs, including the second-generation TKI afatinib [9] and the third-generation TKIs osimertinib [10] and olmutinib [6], has become the main objective of current research focusing on cancer treatment. Nevertheless, approximately 10% of NSCLC patients show primary TKI resistance, and the underlying mechanism remains unclear.

The expression of the proto-oncogene Src is related to tumour development and a poor prognosis because Src regulates signalling pathways that affect the expression of its downstream proteins [11]. Src is a member of the Src family of kinases (SFKs), which are nonreceptor kinases. Under normal conditions, approximately 90%-95% of Src is phosphorylated at the Tyr530 position, which corresponds to a closed and inactive structure. In its activated form, Src is dephosphorylated at Tyr530 and autophosphorylated at Tyr416 in its kinase domain [12]. Mutations in EGFR and its family of related proteins enhance Src expression and activate Src downstream signals through the extracellular regulated protein kinase (ERK), AKT and signal transducer and activator of transcription (STAT) signalling pathways [13]. Src and EGFR show synergistic effects via mutual phosphorylation and activation [14], and their coexpression induces cell transformation [15].

Because of the crosstalk between Src and EGFR, inhibiting Src may improve NSCLC treatment [16]. Several known Src inhibitors, including dasatinib (BMS-354825), saracatinib (AZD0530), and ponatinib (AP24534), have been developed as therapeutic agents, and their effectiveness against solid tumours has been evaluated in clinical trials [17]. Src inhibitors induce apoptosis in various NSCLC cell lines and inhibit cell survival and EGFR-regulated malignant transformation [14]. Thus, inhibiting the Src pathway alone can induce apoptosis, and combining Src inhibitors with gefitinib could further enhance the effects of Src inhibitors on EGFR- and HER2-driven cancers.

This study aims to identify novel compounds less dependent on EGFR status than other currently available compounds to increase the efficacy of lung cancer treatment. In this study, using the Src pY419 enzyme-linked immunosorbent assay (ELISA) as the platform to screen a compound library of more than 400 plant active ingredients, we identified peruvoside (PubChem CID: 12314120) as a candidate inhibitor of Src-EGFR crosstalk. We also investigated the functional mechanism underlying the ability of peruvoside to suppress lung cancer cell progression using *in vitro* and *in vivo* approaches. Our findings may promote the development of new anticancer drugs and therapeutic strategies that are useful to treat lung cancer in the future.

Materials and methods

Cell culture

The human bronchial epithelial cell line BEAS2B (ATCC CRL-9609) and human lung adenocarcinoma cell lines A549 (ATCC CCL-185; EGFR wild-type, TKI resistant) and H1975 (ATCC CRL-5908; EGFR L858R+T790M, TKI resistant) were obtained from the American Type Culture Collection (ATCC; Manassas, VA, USA). The human lung adenocarcinoma cell lines PC9 (EGFR exon 19 deletion, TKI sensitive), PC9/gef (TKI resistant) and H3255 (EGFR L858R, TKI-sensitive) were kind gifts from Dr. Chih-Hsin Yang (National Taiwan University Hospital, Taiwan). Lung cancer cell lines were typically used no more than eight passages after thawing. The cell lines were grown in RPMI (Gibco, Breda, The Netherlands) supplemented with 10% foetal bovine serum (FBS; Gibco) and 1% penicillin/streptomycin at 37°C in a humidified atmosphere of 5% CO_2.

Drug treatment and herbal compound library

The herbal compound library representing a collection of 415 pure products and their derivatives was purchased from Sigma-Aldrich (St. Louis, MO) and ChromaDex (Irvine, CA) and contained a range of alkaloids, diterpenes, pentacyclic triterpenes, sterols, and many other diverse representatives. Peruvoside was purchased from Sigma-Aldrich, and a stock solution of peruvoside was prepared in dimethyl sulfoxide (DMSO) and stored at -20°C. The compound was diluted in fresh medium before each experiment, and the final DMSO concentration was lower than 0.1%. To determine whether peruvoside promotes protein degradation through the ubiquitination pathway, A549 cells were treated with 10 μM MG132, a proteasome inhibitor (Sigma-Aldrich), for 2 h followed by peruvoside (25 nM) for an additional 24 h. The cell lysates were extracted and then subjected to western blot analysis of the specific proteins.

Enzyme-linked immunosorbent assay (ELISA)

To accelerate the screening of the compound library, ELISA (Human Phospho-Src (Y419) DuoSet IC ELISA; R&D Systems, Minneapolis, MN, USA) was performed. The details of the procedures, including plate preparation and signal detection, are described in the manufacturer's instructions. Briefly, A549 cells were seeded at 1.5×10^5 cells per well and then treated with various compounds (10 μM) for 24 h. After protein extraction and quantification, the cell lysates or standards were added to 96-well microplates coated with the diluted capture antibody for 2 h. Next, the detection antibody and streptavidin-HRP (1:2000) were consecutively added to each well. After the samples were incubated with the substrate solution and stop solution, the absorbance was measured at 450 nm (570 nm as the reference) using a multilabel plate reader (Vector^3; Perkin-Elmer, USA). The absorbance at 570 nm was subtracted from the absorbance at 450 nm to calculate the amount of Src phosphorylation.

Western blot analysis

Western blotting was used to examine the phosphorylated and total levels of Src and other related proteins after peruvoside treatment. The detailed procedures were described previously [18]. The EGFR (sc-373746), STAT3 (F-2) (sc-8019), phosphoinositide 3-kinase (PI3K) (sc-1637), phospho-MEK1/2 (Ser 218/Ser 222) (sc-7995), MEK (sc-436), phospho-ERK (Tyr204) (sc-7383), ERK (sc-1647), Paxillin (sc-365174), and p130cas (sc-9963) antibodies were purchased from Santa Cruz Biotechnology, Inc. (Dallas, TX, USA). Phospho-Src (pY419) (44660G), and focal adhesion kinase (FAK) (AHO1272) antibodies were purchased from Invitrogen (Carlsbad, CA, USA). The phospho-AKT (phospho Ser473) (GTX128414) antibody was purchased from GeneTex (Irvine, California, USA). Phospho-EGFR (Tyr1068) (2236), phospho-FAK (Tyr576) (3281), phospho-STAT3 (Tyr705) (9138S), phospho-PI3K (Tyr458) (4228s), phospho-Stress-activated protein kinase (SAPK)/c-Jun N-terminal kinase (JNK) (Thr183/Tyr185) (9255S), SAPK/JNK (9252S), AKT (4691S), phospho-Paxillin (Tyr-118) (2541S), and phospho-p130cas (Tyr410) (4011S) antibodies were purchased from Cell Signalling Technology (Beverly, MA, USA), and the primary antibody to Src was manufactured in our laboratory (ATCC CRL-2651). Monoclonal mouse anti-glyceraldehyde-3-phosphate dehydrogenase (GAPDH) (1:5000; Upstate Biotechnology, Lake Placid, NY, USA) was used as a loading control. The protein expression levels were quantified using ImageJ software (NIH), and all experiments were performed at least three times in duplicate.

Cell viability and proliferation assay

The PrestoBlue (Invitrogen) cell viability reagent was used to evaluate the cytotoxic and proliferative effects of peruvoside after various durations as described previously [19]. Briefly, the tested cell lines were seeded in 96-well plates at a density of 5×10^3 cells/well and incubated for 24 h. Next, the cells were treated with different concentrations of peruvoside for 24, 48, 72 and 96 h. Subsequently, PrestoBlue solution was added to the wells. After a further incubation of 1.5 h, the absorbance was measured at 570 nm (600 nm as the reference) using a multilabel plate reader (Vector^3; Perkin-Elmer, USA).

Colony formation assay

For the anchorage-dependent growth assay, 500 cells were seeded in six-well plates and treated with peruvoside. After one week, the

A549 cells were washed with PBS, fixed with 4% paraformaldehyde, and stained with 0.05% crystal violet. For the anchorage-independent growth assay, A549 cells were seeded at 1 × 10^3 cells per well in soft agar. After solidification, the cells were treated with different concentrations of peruvoside. The cells were incubated for 2 weeks and then stained with 0.5 mg/ml *p*-iodonitrotetrazolium violet. Colonies with a diameter greater than 1 mm were counted under an inverted microscope. The assay was performed as described previously [18].

Cell migration and invasion assays

The motility of cancer cells was measured using Transwell inserts according to our previous study [19]. Briefly, Transwell membranes (8-μm pore size, 6.5-mm diameter; Corning CoStar Corporation) with or without Matrigel coating (2.5 mg/ml; BD Biosciences Discovery Labware) were used for the invasion and migration assays, respectively. Medium with 10% FBS was added to the lower wells of the chambers, and the upper chambers were seeded with 1 × 10^4 (for migration) or 2 × 10^4 (for invasion) A549 cells in serum-free medium. The medium in the upper chambers contained different concentrations of peruvoside (10 and 50 nM); 0 μM comprised 0.1% DMSO (solvent control). After 12 (migration) or 24 h (invasion) of incubation, cells remaining in the upper chamber were removed, and the cells that migrated onto the lower surface of the membranes were fixed with methanol and stained with 20% Giemsa solution (Sigma-Aldrich). The cells were counted under a light microscope. The experiments were performed in triplicate.

In vivo animal studies

Animal experiments were approved by the Institutional Animal Care and Use Committee of National Chung Hsing University (IACUC No. 105-129), and tumorigenesis experiments were performed in mice according to previously described protocols [19]. Six-week-old nude mice (males, 18-20 grams) obtained from the National Laboratory Animal Center, Taipei, Taiwan were housed at six mice per cage. Briefly, 2 × 10^6 A549 cells in 100 μl of PBS were subcutaneously injected into nude mice. When the tumour size reached a volume of 50-100 mm^3, the mice were randomly grouped into peruvoside-treated (n = 6) or untreated groups (n = 6). Peruvoside was dissolved in DMSO and intraperitoneally (i.p.) dosed once daily at 0.1 mg/kg for 4 weeks. After i.p. injection, the mice were monitored every 7 days for tumour appearance. Body weights were collected prior to study initiation and weekly throughout the study. After 4 weeks, the mice were killed, and their tumours were analysed. The tumour volumes were estimated from the calliper-measured lengths (*a*) and widths (*b*) using the formula $V = 0.4 \times ab^2$ [20].

Real-time reverse transcription-PCR (RT-PCR) and immunohistochemical staining

The expression levels of Src and related genes were detected by real-time RT-PCR using an ABI Prism 7300 sequence detection system (Applied Biosystems, Foster, CA). TATA-box-binding protein (TBP) was used as the internal control (GenBank X54993). The detailed procedures and calculations have been described previously [18]. Immunohistochemical staining was used to investigate the level of phosphorylated Src in tumour tissues from nude mice. Briefly, paraffin-embedded tumour tissue sections were treated with rabbit anti-human Src pY419 polyclonal primary antibody (44660G, Invitrogen) followed by incubation with horseradish peroxidase-conjugated anti-rabbit secondary antibody and the enzyme substrate 3,3'-diaminobenzidine. A DAKO EnVision System was used to observe Src activity.

Drug synergy analysis

To elucidate the synergistic effects of peruvoside and gefitinib on gefitinib-resistant lung cancer cells *in vitro* A549 (EGFR wild-type), PC9/gef (EGFR exon19 deletion) and H1975 (EGFR L858R+T790M) cells were treated with various combinations and then subjected to viability assays. The resulting data were further analysed using CalcuSyn software (Biosoft, Cambridge, UK) and the combination index (CI)-isobologram equation, as described previously [21]. CI < 1, CI = 1 and CI > 1 represent the synergistic, additive and antagonistic effects of the indicated compounds, respectively.

Statistical analysis

All *in vitro* experiments were performed at least in triplicate, and the results are presented as the means ± standard deviations where appro-

priate. Statistical analyses were performed using two-tailed Student's t test, and significant differences were defined as *P* values of less than 0.05.

Results

Drug bank screening via the Src pY419 ELISA platform

In our study, the western blotting results showed that Src phosphorylation was highly increased in the NSCLC cell line with wild-type EGFR (A549) compared with that in cell lines with EGFR mutations (H1975 and PC9) (Figure S1). Moreover, previous research indicated that primary resistance of NSCLCs to EGFR TKIs is mostly associated with wild-type EGFR [8]. Hence, the A549 cell line was selected as the most suitable cell line for our ELISA screening. ELISA was performed to determine the inhibitory effect of the 415 pure compounds in the library on Src activity. The screening criteria and procedures of the drug bank are illustrated in Figure S2. Because we were not sure which concentrations of each drug would effectively inhibit Src phosphorylation, we used high concentrations (10 μM) for drug screening. Our strategy was to use 10 μM concentrations for screening potential compounds in the first round. Among 415 compounds, 20 compounds revealed an inhibitory rate of pSrc activity greater than 50%. These compounds were subjected to a second ELISA. After two runs of ELISA screening, only 18 compounds showed a significant inhibitory effect compared with that of the control (Figure S3 and Table S5). Among these compounds, five had more than 50% inhibitory activity on Src phosphorylation and were identified as candidates. Next, lower concentrations were used to observe whether these concentrations still inhibited Src phosphorylation. The A549 lung cancer cell line was treated with drug concentrations of either 1 or 2 μM, and an ELISA was performed. The results showed that three compounds (D6003, L2261 and P7897) could still effectively inhibit Src activity by greater than 50%, even at low concentrations (Figure S4). To focus our efforts, peruvoside (P7897), a cardiac glycoside (CG) with inotropic and chronotropic effects (**Figure 1A**), was selected for further *in vitro* and *in vivo* studies.

Effect of peruvoside treatment on cell viability and Src-related protein phosphorylation

The lung cancer cell line A549 was treated with various concentrations of peruvoside and then subjected to the cytotoxicity assay at 24, 48, 72, and 96 h. The results are presented as the percentage relative to the DMSO-treated control, and the corresponding half maximal inhibitory concentration (IC_{50}) values at each time point are shown in Table S1. The cytotoxicity results at 24 h indicated that cell viability was poorly affected by 10 nM peruvoside, a dose that is approximately equivalent to the IC_{20}. Therefore, to determine the effects of peruvoside on cellular functions in subsequent experiments, we used concentrations no higher than 50 nM (IC_{50}), which are more appropriate concentrations for the following investigations (**Figure 1B**). To determine the inhibitory effects of peruvoside on Src, EGFR and STAT3 phosphorylation, western blotting was performed. Peruvoside inhibited the activation and expression of Src, EGFR and STAT3 in A549 cells at 24 h in a dose- and time-dependent manner (**Figure 1C**). Similar results were obtained in two other lung cancer cell lines: H3255 (**Figure 1D**, left panel) and H1975 (**Figure 1D**, right panel).

Inhibition of EGFR-mutant lung cancer cell viability and proliferation by peruvoside

To identify the cytotoxic effect of peruvoside on EGFR-mutant cell lines, PC9 and PC9/gef cells with exon 19 deletion, H3255 cells harbouring the L858R mutation and H1975 cells harbouring the L858R and T790M mutations were used. The viabilities of TKI-sensitive and TKI-resistant cell lines were significantly inhibited by 50 nM peruvoside at all tested time points (**Figure 2A-D**). Furthermore, the immortalized BEAS-2B human bronchial epithelial cell line was used to evaluate the cytotoxicity of peruvoside. Peruvoside showed lower cytotoxicity in BEAS-2B cells than in cancer cell lines (Figure S5). Additionally, the results from the cytotoxicity assays were analysed using CalcuSyn software (Biosoft, Cambridge, UK) to determine the IC_{50} value in the five NSCLC cell lines and BEAS-2B cells. For example, the 24 h IC_{50} values in A549, PC9, PC9/gef, H3255, H1975 and BEAS-2B cells were 48 nM, 74 nM, 67 nM, 143 nM,

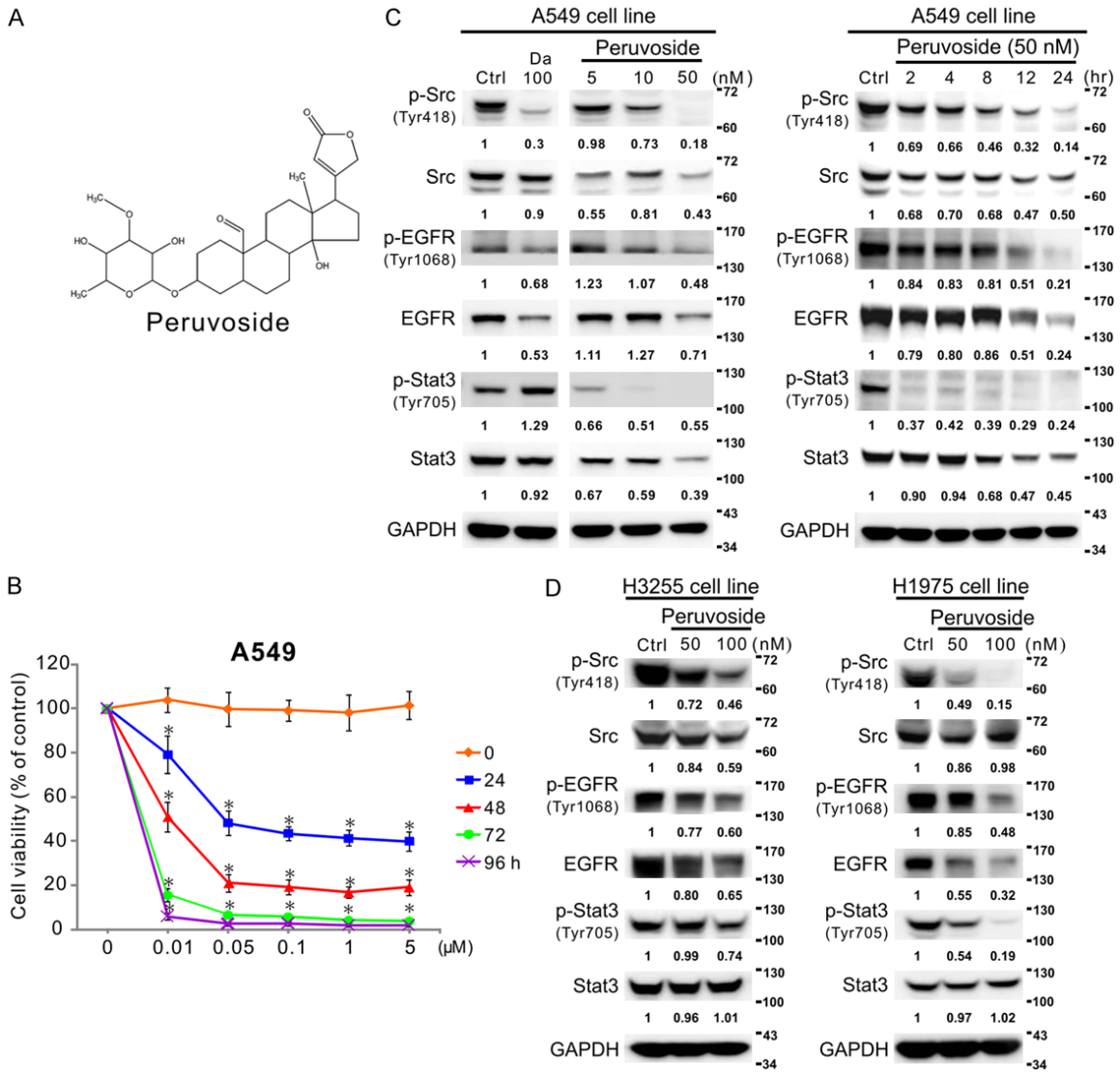

Figure 1. Effects of peruvoside on Src, EGFR and STAT3 expression and the viability of different cell lines. A. Chemical structure of peruvoside. B. Inhibition of A549 cell viability by peruvoside at different concentrations and time points as determined by PrestoBlue staining. The results are presented as percentages of the vehicle control (0 μM, 0.1% DMSO). The IC_{50} values of the designated time points are shown in Table S1. Each experiment was performed independently and in triplicate. *P < 0.05 compared with the vehicle control. C. Inhibition of the protein expression and phosphorylation of Src, EGFR, and STAT3 by peruvoside in A549 cells. Left panel: cells were treated with the indicated concentrations of peruvoside for 24 h and then subjected to western blotting. Right panel: cells were treated with 50 nM peruvoside for the specified time and then subjected to western blotting. D. Inhibition of Src, EGFR, and STAT3 expression and phosphorylation by peruvoside in H3255 (left panel) and H1975 (right panel) cells. The cells were treated with the indicated concentrations of peruvoside for 24 h and then analysed by western blotting. The protein expression levels were quantified by ImageJ software (NIH) and are directly shown below the gel image. Ctrl: 0.1% DMSO; Da100: 100 nM dasatinib as a positive control. GAPDH served as a loading control.

277 nM and 428 nM, respectively (Table S1). Furthermore, we performed statistical analysis and also found that dasatinib significantly inhibited the proliferation of A549 (48, 72, and 96 h) and H3255 (24, 48, 72, and 96 h) lung cancer cells. Moreover, we found that the inhibitory effect of peruvoside was more significant than that of dasatinib in each cell line (**Figure 3A-E**). Therefore, regardless of the EGFR status in the cell line, peruvoside effectively inhibited cell proliferation-even better than dasatinib.

Anticancer effect of peruvoside on cancer cell functions

Colony formation, migration and invasion assays were performed to investigate the antican-

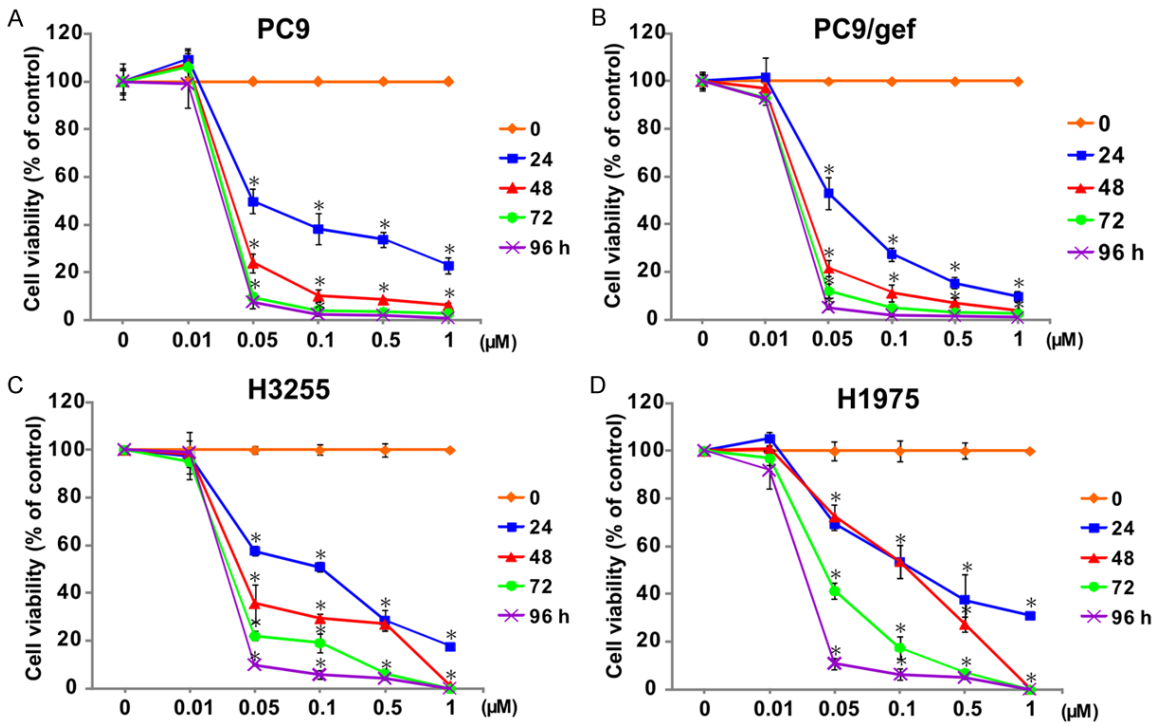

Figure 2. Cytotoxicity of peruvoside in NSCLC cell lines with different EGFR mutation statuses. PC9 (A), PC9/gef (B), H3255 (C) and H1975 (D) cells were treated with various concentrations of peruvoside for 24, 48, 72, 96 h and then subjected to cell viability assays. The results are presented as percentages of the vehicle control (0 μM, 0.1% DMSO). The IC_{50} values of the designated time points are shown in Table S1. Each experiment was performed independently and in triplicate. *P < 0.05 compared with the vehicle control.

cer effects of peruvoside. We demonstrated that peruvoside inhibited the anchorage-dependent growth and anchorage-independent growth of A549 cells (**Figure 4A** and **4B**) in a concentration-dependent manner; notably, a concentration as low as 5 nM was sufficient to inhibit colony formation. To investigate the effects of peruvoside on cell motility, A549 cells were pre-treated with peruvoside for 24 h and then subjected to Transwell migration and invasion assays for 12 h and 24 h, respectively. Peruvoside significantly inhibited the migratory and invasive abilities of cells, even at a low concentration of 10 nM (**Figure 4C** and **4D**).

Suppression of in vivo tumour growth by peruvoside

To further examine the effect of peruvoside *in vivo*, A549 cells were subcutaneously injected into nude mice. The mice were then treated with peruvoside (i.p., 0.1 mg/kg/day, n = 6) or vehicle (n = 6) and observed every 7 days to monitor tumour growth. Twenty-eight days after treatment, the peruvoside-treated group had an average tumour size of 129.9 mm^3 (95% CI = 86-174 mm^3; P = 0.0068), which was significantly smaller than that of the control group (348 mm^3, 95% CI = 189-507 mm^3) (**Figure 5A**). After 4 weeks, the mice were killed, and their tumour sizes were analysed. The tumour weights were also significantly decreased from 0.55 g in the control group to 0.26 g in the peruvoside-treated group (P = 0.0126; **Figure 5B**). To determine the change in Src activity in tumours, the tissues were sectioned and immunostained with human anti-phospho-Src antibody. The immunohistochemistry data indicated that peruvoside significantly decreased levels of phosphorylated Src Y419 in tumour tissues compared with control tissues (**Figure 5C**).

Peruvoside has synergistic effects when used in combination with gefitinib

To evaluate the combined effects of peruvoside and gefitinib on the cells, CI-isobologram

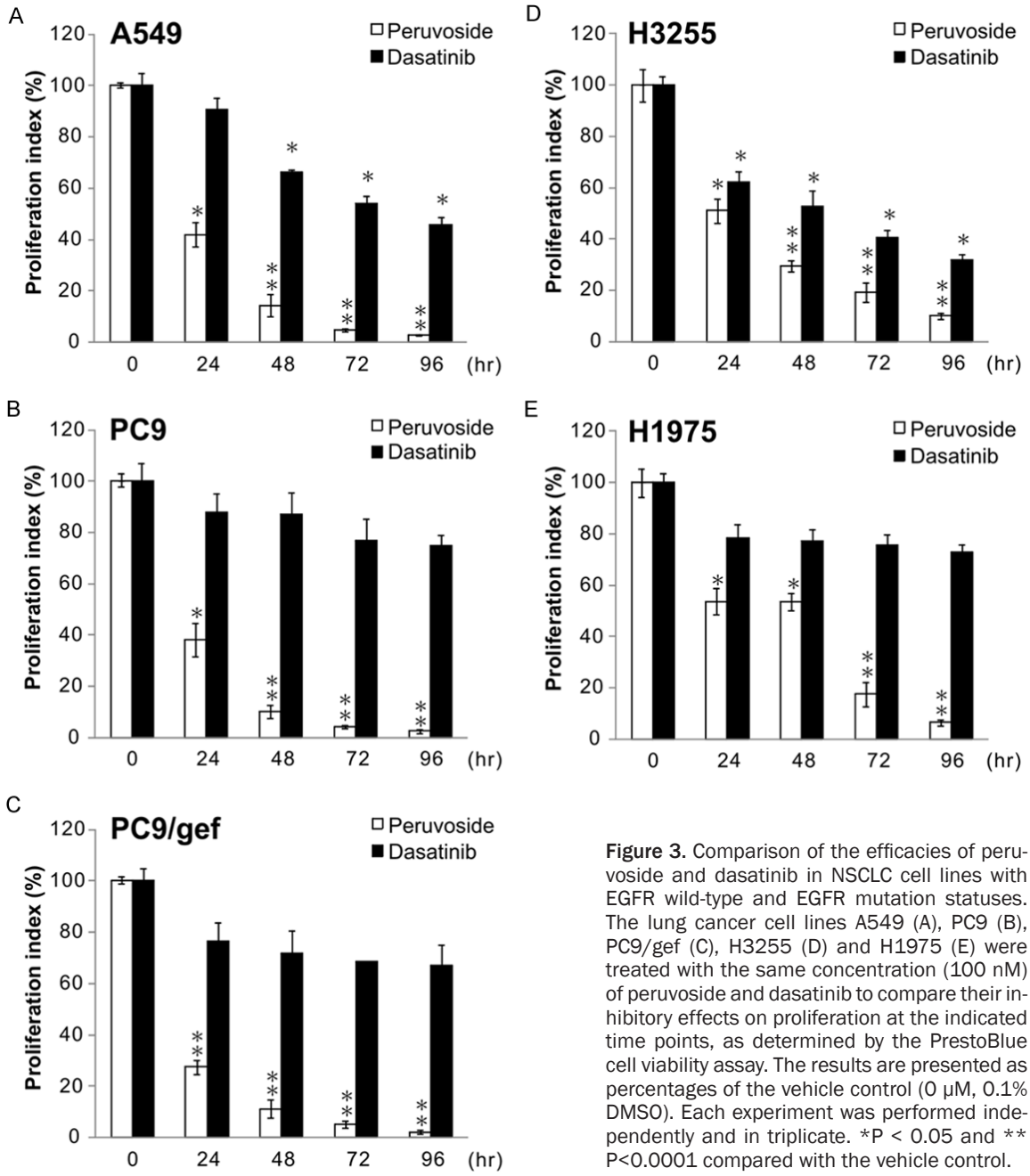

Figure 3. Comparison of the efficacies of peruvoside and dasatinib in NSCLC cell lines with EGFR wild-type and EGFR mutation statuses. The lung cancer cell lines A549 (A), PC9 (B), PC9/gef (C), H3255 (D) and H1975 (E) were treated with the same concentration (100 nM) of peruvoside and dasatinib to compare their inhibitory effects on proliferation at the indicated time points, as determined by the PrestoBlue cell viability assay. The results are presented as percentages of the vehicle control (0 μM, 0.1% DMSO). Each experiment was performed independently and in triplicate. *P < 0.05 and ** P<0.0001 compared with the vehicle control.

analysis was performed based on cell viability. The lung adenocarcinoma cell lines A549, PC9/gef, and H1975 were treated with different combinations of these two compounds for 72 h. The results of the CI-isobologram analysis indicated that peruvoside and gefitinib exerted synergistic effects on A549 (CI: 0.012~0.768), PC9/gef (CI: 0.15~0.915), and H1975 cells (CI: 0.353~0.628) (Tables S2, S3, S4). Specifically, the combination of 0.005, 0.075, or 0.01 μM peruvoside and a low dose of gefitinib (0.01 or 0.05 μM) had synergistic effects on A549 cells (**Figure 5D**, upper panels). Furthermore, the combination of 0.025 or 0.05 μM peruvoside and gefitinib increased the sensitivity of PC9/gef and H1975 cells to gefitinib, even when peruvoside was administered at concentrations as low as 0.01 μM (**Figure 5D**, middle and lower panels). In summary, 0.025 μM and 0.05 μM peruvoside rendered A549, PC9/gef, and H1975 gefitinib-resistant lung cancer cells sensitive to lower concentrations of gefitinib.

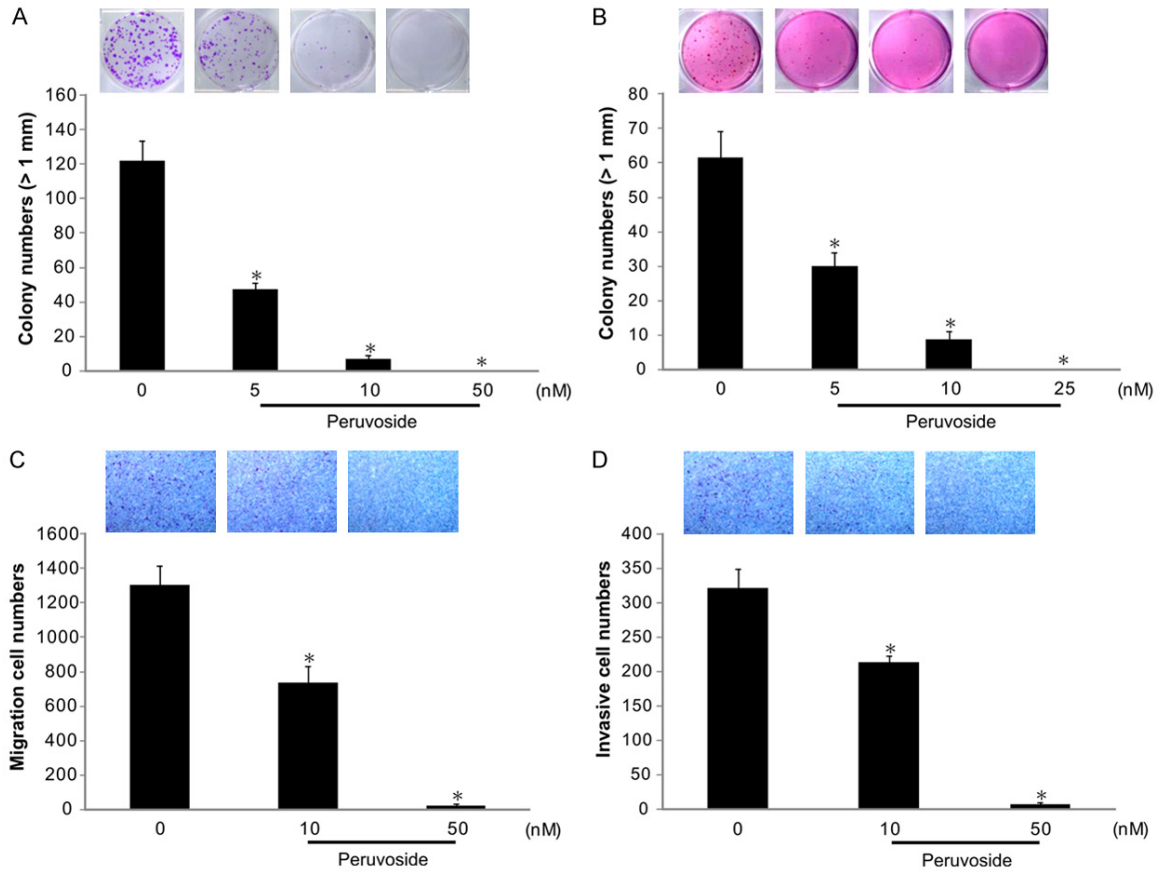

Figure 4. Suppressive effects of peruvoside on anchorage-dependent and anchorage-independent growth and motility. The colony formation assay was used to determine the inhibitory effect of peruvoside on clonogenicity. A. Anchorage-dependent cell growth of the A549 cell line. Colonies with diameters ≥ 1 mm were counted. B. Anchorage-independent cell growth of the A549 cell line. Colonies with diameters ≥1 mm were counted. Each experiment was performed independently and in triplicate. 0 nM: 0.1% DMSO. C. Inhibitory effect of peruvoside on cancer cell migration, as determined by the Transwell assay. D. Inhibitory effect of peruvoside on cancer cell invasion, as measured by the Transwell assay. Each experiment was performed independently and in triplicate. *P < 0.05 compared with the vehicle control.

Effect of peruvoside on Src downstream pathways

To determine the mechanisms by which peruvoside inhibits cancer cell functions, western blotting of previously reported Src-related signalling pathways was performed. These proteins included PI3K and AKT for the survival pathway; MEK and ERK for the proliferation pathway; and FAK, Paxillin, p130 CAS and JNK for the migration and invasion pathways [22]. A549 cells were treated with the indicated concentrations of peruvoside for 24 h, and peruvoside inhibited the phosphorylation of PI3K, AKT, FAK, SAPK/JNK, Paxillin and p130 CAS in these cells. However, the levels of phosphorylated MEK and ERK were not reduced by peruvoside treatment (**Figure 6A**).

In addition to using the EGFR wild-type A549 cell line, we used the EGFR-mutant H3255 and H1975 cell lines to evaluate whether peruvoside can effectively inhibit the phosphorylation of these proteins in NSCLC cell lines with TKI-sensitive or TKI-resistant EGFR mutations, respectively. These two cell lines were treated with sublethal doses of peruvoside (50 nM and 100 nM) for 24 h and then subjected to western blotting. In H3255 cells, the proteins and pathways affected by peruvoside were similar to those in A549 cells (**Figure 6B**), except for p-MEK, p-ERK and Paxillin. Furthermore, in H1975 cells, peruvoside suppressed the phosphorylation of PI3K, AKT, MEK, ERK, FAK, SAPK/JNK, Paxillin and p130 CAS (**Figure 6C**). Overall, the results in the three cell lines also

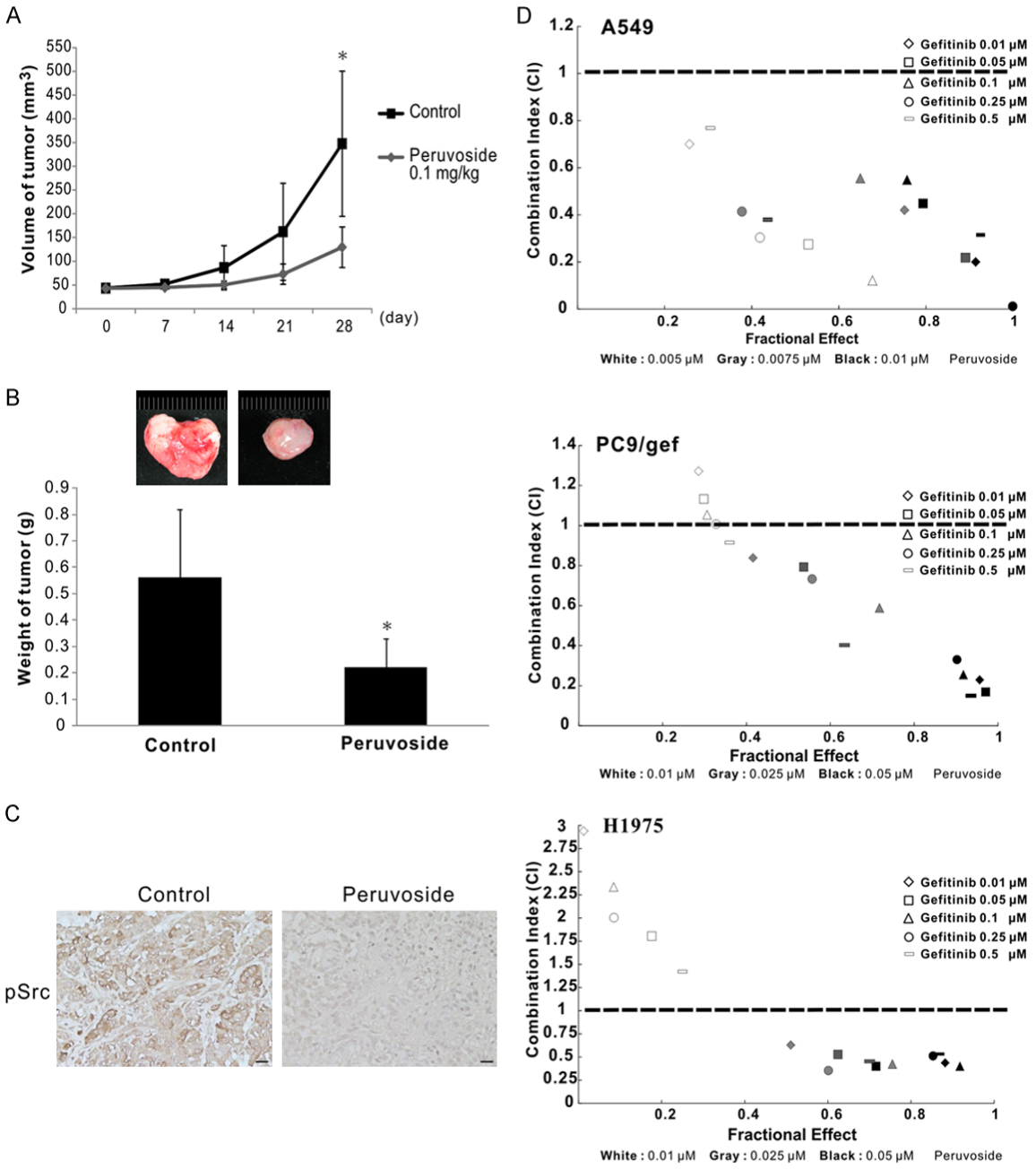

Figure 5. Effects of peruvoside on tumour growth and drug synergism. The indicated number of live A549 cells was subcutaneously injected into mice divided into vehicle-treated (n = 6) and drug-treated groups (n = 6). A. The tumour volumes were measured every 7 days. B. Peruvoside decreased the tumour weight. The data are presented as the means ± standard deviations. C. The p-Src level and distribution in murine tumour tissues were determined by immunohistochemical staining and observed under a light microscope (400 × magnification). The control represents 0.1% DMSO, and peruvoside was administered at 0.1 mg/kg. The scale bars represent 20 μm. *P < 0.05 compared with the vehicle control (0.1% DMSO). D. Synergistic effects of peruvoside and gefitinib on lung cancer cell lines, as determined by the cell viability assay. The indicated combinations of peruvoside and gefitinib were used to treat the gefitinib-resistant lung adenocarcinoma cell lines A549, PC9/gef and H1975 for 72 h. The CI was calculated using CalcuSyn software. Each experiment was performed independently and was repeated three times.

showed that the phosphorylation of Src and some Src-related proteins, such as EGFR, STAT3 and FAK, was downregulated by peruvoside (**Figures 1** and **6**).

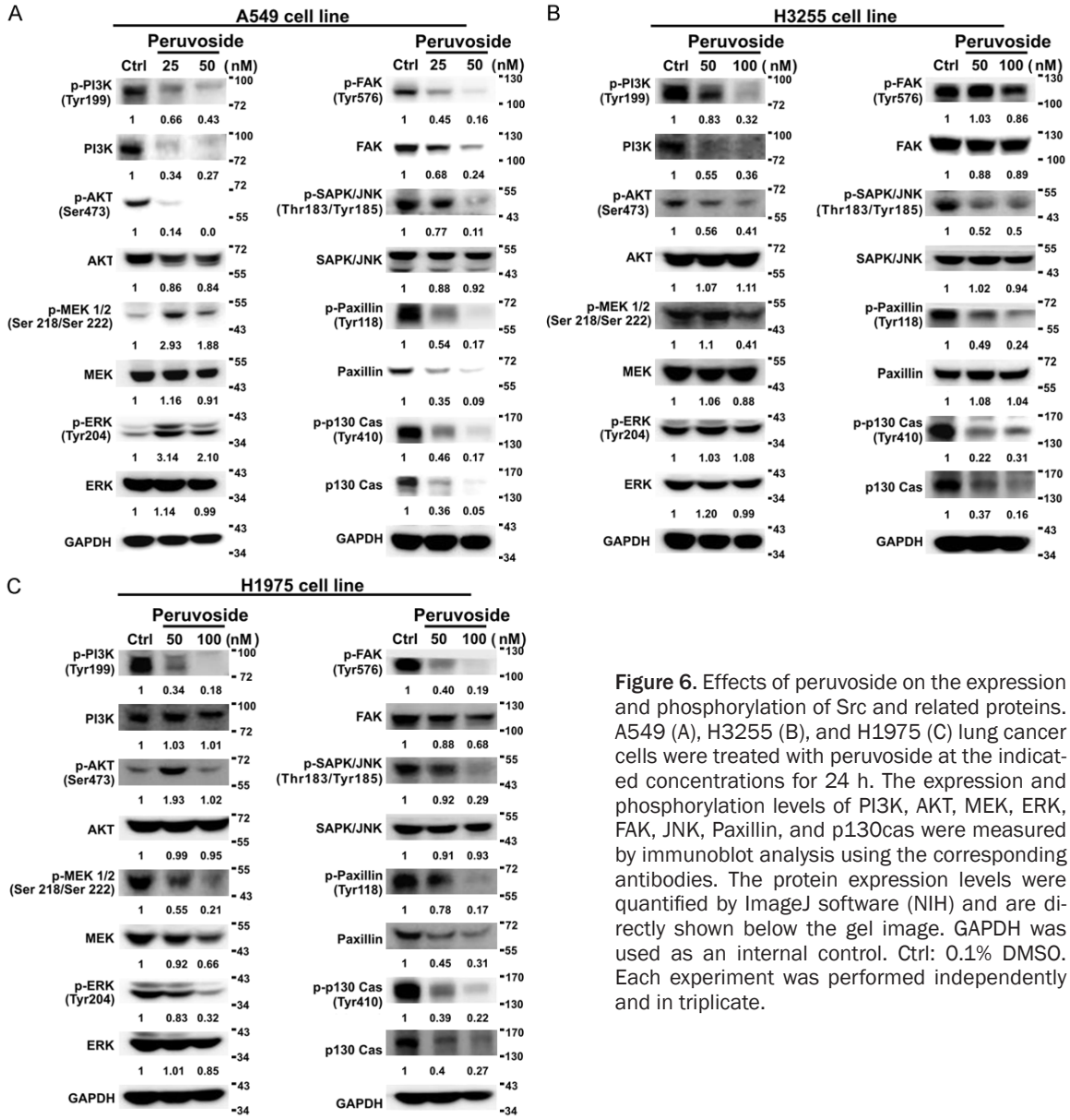

Figure 6. Effects of peruvoside on the expression and phosphorylation of Src and related proteins. A549 (A), H3255 (B), and H1975 (C) lung cancer cells were treated with peruvoside at the indicated concentrations for 24 h. The expression and phosphorylation levels of PI3K, AKT, MEK, ERK, FAK, JNK, Paxillin, and p130cas were measured by immunoblot analysis using the corresponding antibodies. The protein expression levels were quantified by ImageJ software (NIH) and are directly shown below the gel image. GAPDH was used as an internal control. Ctrl: 0.1% DMSO. Each experiment was performed independently and in triplicate.

Peruvoside reduced the mRNA expression of Src and related pathways

The expression levels of Src and some of its related proteins were decreased in peruvoside-treated cells compared with control cells (**Figures 1** and **6**). The reduced protein levels could be explained by alterations in transcription and protein stability. Therefore, real-time PCR was performed to investigate the effect of peruvoside on the transcriptional regulation of the genes tested in this study. The mRNA expression levels of EGFR, Src, STAT3 and FAK were significantly downregulated by peruvoside, even when the drug was administered at a relatively low concentration (25 nM) (**Figure 7A**). However, to explore whether the ubiquitin-proteasome system plays a role in peruvoside-induced reductions in protein expression, the proteasome inhibitor MG132 was added to cell cultures. Peruvoside decreased the expression of the tested proteins as described previously in this study, but cotreatment with MG132 did not restore their expression compared with that in the vehicle control (**Figure 7B**). Therefore, we speculate that the protein reduction caused by peruvoside occurs via regulation of RNA levels. However, further investigations are needed to clarify the detailed regulatory mechanisms.

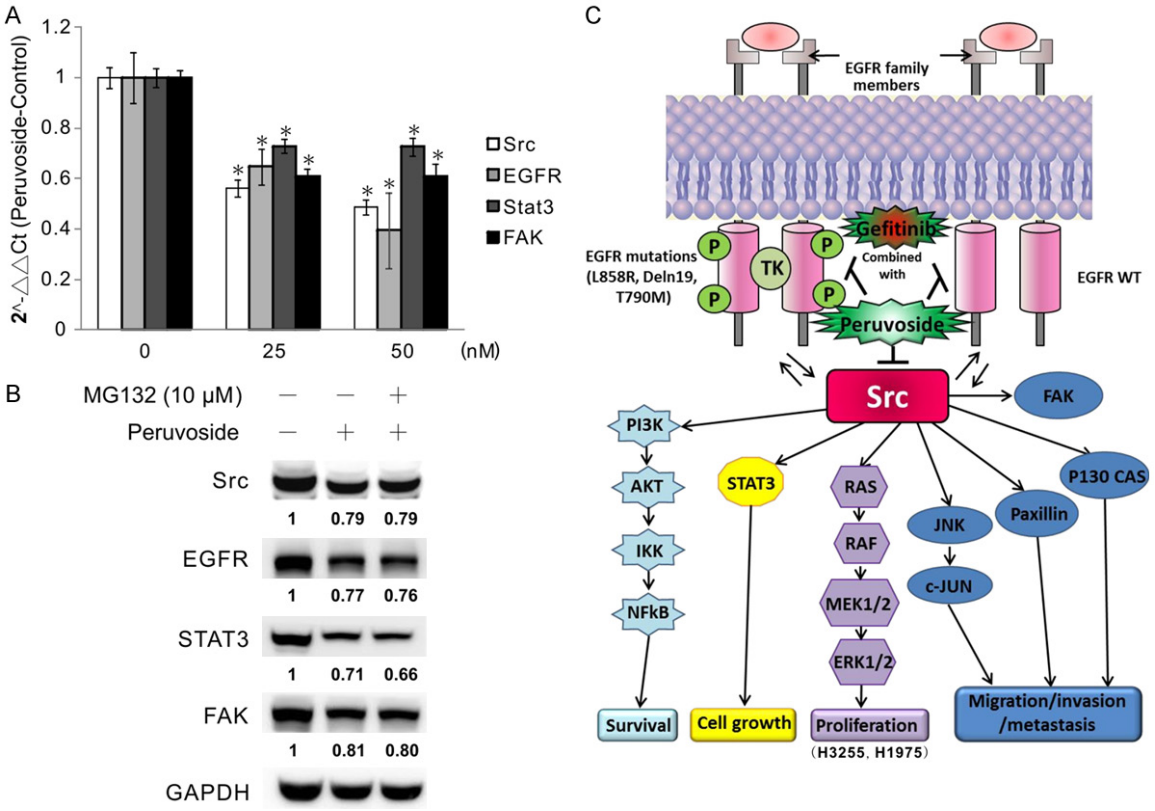

Figure 7. Peruvoside inhibits Src and Src-related gene transcription. A. Repressive effects of peruvoside on Src, EGFR, STAT3, and FAK transcription in A549 cells, as determined by real-time RT-PCR. The relative gene expression levels were calculated using the comparative CT method ($2^{-\Delta\Delta CT}$). TBP: internal control. Each experiment was performed independently and in triplicate. *P < 0.05 compared with the control (0 nM: 0.1% DMSO). B. Role of the ubiquitin-proteasome system in peruvoside-mediated decreases in protein expression. MG132 and/or peruvoside was administered to A549 cells for 24 h before the cells were subjected to western blotting. GAPDH served as a loading control. Protein expression was quantified with ImageJ software (NIH), and the results are shown directly below the gel graph. C. A hypothetical model illustrating the role of peruvoside in suppressing lung cancer tumorigenesis. Peruvoside significantly suppressed the phosphorylation of Src, EGFR, and STAT3 in different NSCLC cell lines (A549, H3255 and H1975 cells) regardless of their EGFR mutation status and had a synergistic effect when combined with gefitinib. Furthermore, the inhibitory effects of peruvoside on lung cancer progression might be attributed to its ability to regulate multiple proteins, including Src, PI3K, JNK, Paxillin, p130cas, and EGFR. By combining these effects, peruvoside can effectively inhibit tumorigenesis.

Discussion

The proto-oncogene c-Src is a non-receptor tyrosine kinase that plays a key role in multiple signalling pathways to regulate cell growth and metastasis in several cancer types [23]. The deregulation of its activity or expression is also related to drug resistance in cancer patients and is associated with poor prognoses [24]. ELISA is widely used as a diagnostic and analytical tool in clinical practice and basic research to detect and quantify specific antigens, proteins or antibodies in a given sample [25]. Moreover, ELISA has several advantages over other screening techniques because of its simplicity, selectivity, and sensitivity. In this study, using Src pY419 ELISA as the platform to screen a compound library with more than 400 plant active ingredients, we found that peruvoside is a potential Src inhibitor that significantly inhibits its NSCLC cell functions *in vitro* and tumorigenesis *in vivo*. Moreover, we determined that peruvoside has a synergistic effect when used in combination with gefitinib.

In addition, we found that 4 drugs among top 5 candidates were in the CG family of medications. CGs belong to a class of organic compounds comprising a sugar (glycoside) and an aglycone (steroid) moiety. The steroid nucleus

consists of four fused rings to which other functional groups such as methyl, hydroxyl, and aldehyde groups can be attached to influence the biological activity of the molecule [26]. The main structure of all four drugs corresponded to CGs, except that the steroid molecules were attached to different sugar (glycosides) groups. These drugs are used to treat cardiac disorders, such as congestive heart failure, ischaemia and cardiac arrhythmia [27]. Interestingly, in recent years, several studies have revealed that some CGs possess potent anticancer effects in various cancers [18, 28]. These results also suggested that CGs could be useful for anticancer therapy.

Peruvoside, a CG, is a natural ingredient extracted from oleander seeds. Peruvoside has been shown to have antiproliferative and anticancer effects by regulating the expression of various key proteins involved in cell cycle arrest, caspase activation and autophagic cell death in several cancers, including myeloid leukaemia, breast cancer and lung cancer cells [29-31]. Furthermore, previous studies have indicated that peruvoside inhibits AKT phosphorylation and β-catenin expression in H460 lung cancer cells (EGFR wild-type) [31] and induces autophagy and apoptosis via mitogen-activated protein kinase (MAPK), Wnt/β-catenin and mammalian target of rapamycin (mTOR) signalling in A549 lung cancer cells (EGFR wild-type) [32]. However, these studies did not investigate the effect of peruvoside on NSCLC with EGFR-activating mutations or acquired resistance EGFR mutations, the Src-EGFR-related signalling pathways involved, or its effect on tumorigenesis *in vivo*. Moreover, the functional role of peruvoside in cancer and the mechanism underlying its antitumour activity are still largely unknown. Here, we elucidated the multifaceted role of peruvoside in NSCLC and the signalling pathways in which it may be involved. To our knowledge, this is the first study to indicate that peruvoside can inhibit NSCLC progression by regulating multiple Src-related signalling pathways.

EGFR is overexpressed in approximately 40%-80% of NSCLC tumours; therefore, EGFR activity and mutations that can trigger downstream signalling pathways are important factors in lung cancer treatment and must be considered by clinicians when managing this disease [33]. Similar to EGFR, c-Src is overexpressed in many types of cancer and is often co-overexpressed with EGFR in several types of tumours, including carcinomas of the colon, breast, and lung [15]. A previous study showed that Src inhibitors not only suppress Src activity but also inhibit EGFR tyrosine kinase activation and downstream signalling pathways. Moreover, depending on the EGFR/Ras mutational profile, different Src inhibitors may exhibit divergent anticancer effects in NSCLCs [34]. Therefore, Src can serve as a therapeutic target to improve NSCLC treatment [14]. The Src inhibitor dasatinib has been approved for clinical use in patients with chronic myeloid leukaemia (CML) [35] and can improve the efficacy of cetuximab and cisplatin in triple-negative breast cancer (TNBC) when used in combination [36]. Moreover, dasatinib was recently shown to be a multikinase inhibitor that affects the STAT5, c-kit, and platelet-derived growth factor receptor (PDGFR) pathways [37]. However, similar to gefitinib, dasatinib cannot inhibit the growth of NSCLC cells with wild-type EGFR (A549) or a T790M mutation (H1975) [38]. Compared to dasatinib, peruvoside exerted cytotoxic effects on all NSCLC cell lines tested, namely A549, PC9, PC9/gef, H3255 and H1975 cells, independent of their EGFR mutation status. Furthermore, a comparison of the IC_{50} values among cell lines after 24 hours of peruvoside treatment revealed that the IC_{50} value of BEAS-2B cells is 2-10-fold higher than that of various other cancer cells. Moreover, peruvoside treatment below the IC_{50} value for 24 hours had an inhibitory effect in most of our experiments. These data show that peruvoside is relatively less toxic to BEAS-2B cells than to other cancer cells in this study.

c-Src has been reported to bind to EGFR and phosphorylate Y845, resulting in the activation of various downstream pathways [39]. Therefore, c-Src and activated EGFR cooperate to induce cell transformation, a process that is critical for EGFR-mediated oncogenesis [40]. Because of the crosstalk between Src and EGFR, inhibiting the activity of both proteins may facilitate the successful treatment of NSCLC patients either without EGFR-activating mutations or with acquired resistance mutations. Previous studies have shown that inhibiting c-Src kinase activity sensitizes EGFR-TKI-resistant cells and significantly decreases AKT

activation, cell survival and migration, indicating that Src inhibitors might overcome resistance to EGFR inhibitors in lung cancer cells [41]. Thus, the effects of combination therapy comprising dasatinib and EGFR TKIs (erlotinib, gefitinib and afatinib) on NSCLC have been investigated in several clinical trials in recent years [42, 43]. However, these phase I/II clinical trials did not obtain ideal results because NSCLC patients with acquired EGFR-TKI-resistant mutations or wild-type EGFR showed minimal or no clinical response [42, 44]. Our data indicated that peruvoside significantly sensitized gefitinib-resistant lung adenocarcinoma cells (A549, PC9/gef, and H1975) to gefitinib treatment *in vitro*, indicating that this compound may reduce the required gefitinib dose, enhance gefitinib efficacy, decrease targeted therapy costs and minimize patient loads. These findings suggest that peruvoside is a new candidate compound that can be used in place of dasatinib in combination therapy regimens comprising one of the two kinase inhibitors.

Src has been identified as an important oncogenic driver of many signalling pathways to enhance cancer cell motility, tumorigenesis, angiogenesis, and metastasis [22]. Among these pathways, some have been demonstrated to modulate cancer progression, including the PI3K/AKT, STAT3, MEK/ERK, JNK, FAK, Paxillin, and p130cas pathways [23]. The PI3K/AKT pathway can be activated by EGFR and Src, leading to increased survival and aberrant cell cycle progression [45]. Our data showed that peruvoside inhibits the activity of Src and EGFR as well as the phosphorylation and expression of PI3K in EGFR-mutant (H3255 and H1975) and wild-type (A549) cells. FAK-Src signalling via Paxillin, ERK, and p130cas regulates actin cytoskeletal reorganization to promote cell migration [46]. Furthermore, JNK is the transcriptional regulator of matrix metalloproteinase (MMP)-2 and MMP-9; thus, JNK activation can lead to proteolysis and increased cell invasion [47]. Our data revealed that peruvoside significantly represses the phosphorylation or protein expression of FAK, JNK, Paxillin, and p130cas in H3255, H1975 and A549 cells, leading to reductions in cancer cell invasion and migration. A previous study showed that MEK and ERK might be involved in the Src-related signalling pathway to increase cell proliferation [48]. In this study, peruvoside decreased the levels of phosphorylated MEK and/or ERK in the indicated cell lines but promoted their levels in A549 cells. Similar results were reported in a previous work [18], which suggested that peruvoside affects other signalling pathways, growth factors or protein kinases to inhibit cell growth in a certain cell line. Additionally, we found that the reductions in certain proteins caused by peruvoside may be due to its effect on transcriptional regulation rather than increased ubiquitination, which is often observed with antitumour drugs such as palbociclib (a CDK inhibitor) and fludarabine (premature transcription chain terminator) [49].

In our previous studies, we found a novel potential compound, AC-93253 iodide that can inhibit NSCLC cell growth and motility by regulating multiple Src-related pathways [19]. However, there are many differences between this compound and peruvoside. First, the methods used to identify these novel compounds that could inhibit Src phosphorylation were different. AC-93253 iodide was found using molecular docking with the LOPAC compound library, and peruvoside was selected using an ELISA from more than 400 active plant ingredients. Second, these two drugs have different origins and classifications. AC-93253 functions similar to retinoid acid (RA) and is a cell permeable, subtype-selective RAR (RAR-α) agonist [50]. Previous studies have indicated that AC-93253 is a novel inhibitor of the class III histone deacetylase SIRT2 that can selectively induce cytotoxicity in cancer cells [51] and affect the expression of a variety of genes important for chemoresistance acquisition and disease progression in melanoma cells [52]. Peruvoside is a CG extracted from oleander seeds. This drug is used to treat cardiac disorders, such as congestive heart failure, ischaemia and cardiac arrhythmia [27]. Third, the mechanism of target protein reduction by these compounds is different. The ability of AC-93253 iodide to decrease mRNA expression levels and increase protein degradation may be attributable to its effects on the ubiquitin-proteasome pathway. The protein reduction caused by peruvoside occurs *via* transcriptional regulation.

In summary, our findings reveal that peruvoside may directly or indirectly affect the expression of Src and downstream or related proteins, thereby inhibiting cancer progression. However, we

cannot rule out the possibility that peruvoside may affect multiple targets. Recently, based on the effects of drugs on multiple target to induce different anticancer responses, the concept of polypharmacology has been developed [53]. Multi-target drugs can treat diseases more effectively than single-target drugs, regardless of whether these multi-target drugs are used alone or in combination with other agents, and multi-target agents are expected to provide more efficacious and safer therapeutic solutions that are less prone to drug resistance phenomena [54]. For example, sorafenib, an inhibitor of vascular endothelial growth factor receptor (VEGFR), PDGFR, KIT, Fms-like tyrosine kinase 3 (FLT3), and RAF, was recently confirmed in clinical trials for its effectiveness in patients with advanced gastrointestinal stromal tumours [55]. Moreover, the safety and efficacy of anlotinib, a novel multi-target TKI that inhibits VEGFR2/3, fibroblast growth factor receptor (FGFR)1-4, PDGFR α/β, c-Kit, and Ret [56], in patients with refractory advanced NSCLC have been verified in a randomized phase II trial.

Conclusion

We found that peruvoside may have multi-target inhibitory effects on NSCLC (**Figure 7C**) and may exert a synergistic effect when combined with gefitinib. These results indicate that peruvoside has potential as a treatment method for cancer. Therefore, whether peruvoside is used alone or in combination with other drugs may be the basis for future therapies and should be evaluated in future drug development studies.

Acknowledgements

This study was supported by grants from the Ministry of Science and Technology, Taiwan, R.O.C. (MOST 103-2314-B-005-001-MY3 and MOST 107-2314-B-005-003-MY3) and Taichung Veterans General Hospital and National Chung-Hsing University (TCVGH-NCHU-1087-609).

Disclosure of conflict of interest

None.

Address correspondence to: Jeremy JW Chen, Institute of Biomedical Sciences, National Chung Hsing University, No. 145, Xingda Rd., South District, Taichung 40227, Taiwan. Tel: +886-4-22840896 Ext. 125; Fax: 886-4-22853469; E-mail: jwchen@dragon.nchu.edu.tw

References

[1] Siegel RL, Miller KD and Jemal A. Cancer statistics, 2020. CA Cancer J Clin 2020; 70: 7-30.

[2] Sequist LV, Heist RS, Shaw AT, Fidias P, Rosovsky R, Temel JS, Lennes IT, Digumarthy S, Waltman BA, Bast E, Tammireddy S, Morrissey L, Muzikansky A, Goldberg SB, Gainor J, Channick CL, Wain JC, Gaissert H, Donahue DM, Muniappan A, Wright C, Willers H, Mathisen DJ, Choi NC, Baselga J, Lynch TJ, Ellisen LW, Mino-Kenudson M, Lanuti M, Borger DR, Iafrate AJ, Engelman JA and Dias-Santagata D. Implementing multiplexed genotyping of non-small-cell lung cancers into routine clinical practice. Ann Oncol 2011; 22: 2616-2624.

[3] Ding L, Getz G, Wheeler DA, Mardis ER, McLellan MD, Cibulskis K, Sougnez C, Greulich H, Muzny DM, Morgan MB, Fulton L, Fulton RS, Zhang Q, Wendl MC, Lawrence MS, Larson DE, Chen K, Dooling DJ, Sabo A, Hawes AC, Shen H, Jhangiani SN, Lewis LR, Hall O, Zhu Y, Mathew T, Ren Y, Yao J, Scherer SE, Clerc K, Metcalf GA, Ng B, Milosavljevic A, Gonzalez-Garay ML, Osborne JR, Meyer R, Shi X, Tang Y, Koboldt DC, Lin L, Abbott R, Miner TL, Pohl C, Fewell G, Haipek C, Schmidt H, Dunford-Shore BH, Kraja A, Crosby SD, Sawyer CS, Vickery T, Sander S, Robinson J, Winckler W, Baldwin J, Chirieac LR, Dutt A, Fennell T, Hanna M, Johnson BE, Onofrio RC, Thomas RK, Tonon G, Weir BA, Zhao X, Ziaugra L, Zody MC, Giordano T, Orringer MB, Roth JA, Spitz MR, Wistuba, II, Ozenberger B, Good PJ, Chang AC, Beer DG, Watson MA, Ladanyi M, Broderick S, Yoshizawa A, Travis WD, Pao W, Province MA, Weinstock GM, Varmus HE, Gabriel SB, Lander ES, Gibbs RA, Meyerson M and Wilson RK. Somatic mutations affect key pathways in lung adenocarcinoma. Nature 2008; 455: 1069-1075.

[4] Pao W. New approaches to targeted therapy in lung cancer. Proc Am Thorac Soc 2012; 9: 72-73.

[5] Ettinger DS. Clinical implications of EGFR expression in the development and progression of solid tumors: focus on non-small cell lung cancer. Oncologist 2006; 11: 358-373.

[6] Juan O and Popat S. Treatment choice in epidermal growth factor receptor mutation-positive non-small cell lung carcinoma: latest evidence and clinical implications. Ther Adv Med Oncol 2017; 9: 201-216.

[7] Wang J, Wang B, Chu H and Yao Y. Intrinsic resistance to EGFR tyrosine kinase inhibitors in advanced non-small-cell lung cancer with acti-

vating EGFR mutations. Onco Targets Ther 2016; 9: 3711-3726.
[8] Gazdar AF. Activating and resistance mutations of EGFR in non-small-cell lung cancer: role in clinical response to EGFR tyrosine kinase inhibitors. Oncogene 2009; 28 Suppl 1: S24-31.
[9] Park K, Tan EH, O'Byrne K, Zhang L, Boyer M, Mok T, Hirsh V, Yang JC, Lee KH, Lu S, Shi Y, Kim SW, Laskin J, Kim DW, Arvis CD, Kolbeck K, Laurie SA, Tsai CM, Shahidi M, Kim M, Massey D, Zazulina V and Paz-Ares L. Afatinib versus gefitinib as first-line treatment of patients with EGFR mutation-positive non-small-cell lung cancer (LUX-Lung 7): a phase 2B, open-label, randomised controlled trial. Lancet Oncol 2016; 17: 577-589.
[10] Remon J, Menis J, Hasan B, Peric A, De Maio E, Novello S, Reck M, Berghmans T, Wasag B, Besse B and Dziadziuszko R. The APPLE trial: feasibility and activity of AZD9291 (Osimertinib) treatment on positive PLasma T790M in EGFR-mutant NSCLC patients. EORTC 1613. Clin Lung Cancer 2017; 18: 583-588.
[11] Summy JM and Gallick GE. Src family kinases in tumor progression and metastasis. Cancer Metastasis Rev 2003; 22: 337-358.
[12] Roskoski R Jr. Src protein-tyrosine kinase structure and regulation. Biochem Biophys Res Commun 2004; 324: 1155-1164.
[13] Chung BM, Dimri M, George M, Reddi AL, Chen G, Band V and Band H. The role of cooperativity with Src in oncogenic transformation mediated by non-small cell lung cancer-associated EGF receptor mutants. Oncogene 2009; 28: 1821-1832.
[14] Leung EL, Tam IY, Tin VP, Chua DT, Sihoe AD, Cheng LC, Ho JC, Chung LP and Wong MP. SRC promotes survival and invasion of lung cancers with epidermal growth factor receptor abnormalities and is a potential candidate for molecular-targeted therapy. Mol Cancer Res 2009; 7: 923-932.
[15] Ishizawar R and Parsons SJ. c-Src and cooperating partners in human cancer. Cancer Cell 2004; 6: 209-214.
[16] Zhang J, Kalyankrishna S, Wislez M, Thilaganathan N, Saigal B, Wei W, Ma L, Wistuba, II, Johnson FM and Kurie JM. SRC-family kinases are activated in non-small cell lung cancer and promote the survival of epidermal growth factor receptor-dependent cell lines. Am J Pathol 2007; 170: 366-376.
[17] Belli S, Esposito D, Servetto A, Pesapane A, Formisano L and Bianco R. c-Src and EGFR inhibition in molecular cancer therapy: what else can we improve? Cancers (Basel) 2020; 12: 1489.
[18] Lin SY, Chang HH, Lai YH, Lin CH, Chen MH, Chang GC, Tsai MF and Chen JJ. Digoxin suppresses tumor malignancy through inhibiting multiple Src-related signaling pathways in non-small cell lung cancer. PLoS One 2015; 10: e0123305.
[19] Lai YH, Lin SY, Wu YS, Chen HW and Chen JJW. AC-93253 iodide, a novel Src inhibitor, suppresses NSCLC progression by modulating multiple Src-related signaling pathways. J Hematol Oncol 2017; 10: 172.
[20] Conway TF Jr, Sabel MS, Sugano M, Frelinger JG, Egilmez NK, Chen F and Bankert RB. Growth of human tumor xenografts in SCID mice quantified using an immunoassay for tumor marker protein in serum. J Immunol Methods 2000; 233: 57-65.
[21] Chou TC and Talalay P. Quantitative analysis of dose-effect relationships: the combined effects of multiple drugs or enzyme inhibitors. Adv Enzyme Regul 1984; 22: 27-55.
[22] Sirvent A, Benistant C and Roche S. Oncogenic signaling by tyrosine kinases of the SRC family in advanced colorectal cancer. Am J Cancer Res 2012; 2: 357-371.
[23] Wheeler DL, Iida M and Dunn EF. The role of Src in solid tumors. Oncologist 2009; 14: 667-678.
[24] Peiro G, Ortiz-Martinez F, Gallardo A, Perez-Balaguer A, Sanchez-Paya J, Ponce JJ, Tibau A, Lopez-Vilaro L, Escuin D, Adrover E, Barnadas A and Lerma E. Src, a potential target for overcoming trastuzumab resistance in HER2-positive breast carcinoma. Br J Cancer 2014; 111: 689-695.
[25] Gan SD and Patel KR. Enzyme immunoassay and enzyme-linked immunosorbent assay. J Invest Dermatol 2013; 133: e12.
[26] Botelho AFM, Pierezan F, Soto-Blanco B and Melo MM. A review of cardiac glycosides: structure, toxicokinetics, clinical signs, diagnosis and antineoplastic potential. Toxicon 2019; 158: 63-68.
[27] Patel S. Plant-derived cardiac glycosides: role in heart ailments and cancer management. Biomed Pharmacother 2016; 84: 1036-1041.
[28] Reddy D, Kumavath R, Barh D, Azevedo V and Ghosh P. Anticancer and antiviral properties of cardiac glycosides: a review to explore the mechanism of actions. Molecules 2020; 25: 3596.
[29] Feng Q, Leong WS, Liu L and Chan WI. Peruvoside, a cardiac glycoside, induces primitive myeloid leukemia cell death. Molecules 2016; 21: 534.
[30] Kaushik V, Azad N, Yakisich JS and Iyer AK. Antitumor effects of naturally occurring cardiac glycosides convallatoxin and peruvoside on human ER+ and triple-negative breast cancers. Cell Death Discov 2017; 3: 17009.
[31] Kaushik V, Yakisich JS, Azad N, Kulkarni Y, Venkatadri R, Wright C, Rojanasakul Y and Iyer

AKV. Anti-tumor effects of cardiac glycosides on human lung cancer cells and lung tumorspheres. J Cell Physiol 2017; 232: 2497-2507.
[32] Reddy D, Kumavath R, Tan TZ, Ampasala DR and Kumar AP. Peruvoside targets apoptosis and autophagy through MAPK Wnt/beta-catenin and PI3K/AKT/mTOR signaling pathways in human cancers. Life Sci 2020; 241: 117147.
[33] Sharma SV and Settleman J. Oncogene addiction: setting the stage for molecularly targeted cancer therapy. Genes Dev 2007; 21: 3214-3231.
[34] Formisano L, D'Amato V, Servetto A, Brillante S, Raimondo L, Di Mauro C, Marciano R, Orsini RC, Cosconati S, Randazzo A, Parsons SJ, Montuori N, Veneziani BM, De Placido S, Rosa R and Bianco R. Src inhibitors act through different mechanisms in non-small cell lung cancer models depending on EGFR and RAS mutational status. Oncotarget 2015; 6: 26090-26103.
[35] Ottmann O, Saglio G, Apperley JF, Arthur C, Bullorsky E, Charbonnier A, Dipersio JF, Kantarjian H, Khoury HJ, Kim DW, Healey D, Strauss L and Cortes JE. Long-term efficacy and safety of dasatinib in patients with chronic myeloid leukemia in accelerated phase who are resistant to or intolerant of imatinib. Blood Cancer J 2018; 8: 88.
[36] Kim EM, Mueller K, Gartner E and Boerner J. Dasatinib is synergistic with cetuximab and cisplatin in triple-negative breast cancer cells. J Surg Res 2013; 185: 231-239.
[37] Hoehn D, Cortes JE, Medeiros LJ, Jabbour EJ, Hidalgo JE, Kanagal-Shamanna R and Bueso-Ramos CE. Multiparameter analysis of off-target effects of dasatinib on bone homeostasis in patients with newly diagnosed chronic myelogenous leukemia. Clin Lymphoma Myeloma Leuk 2016; 16 Suppl: S86-92.
[38] Song L, Morris M, Bagui T, Lee FY, Jove R and Haura EB. Dasatinib (BMS-354825) selectively induces apoptosis in lung cancer cells dependent on epidermal growth factor receptor signaling for survival. Cancer Res 2006; 66: 5542-5548.
[39] Sato K. Cellular functions regulated by phosphorylation of EGFR on Tyr845. Int J Mol Sci 2013; 14: 10761-10790.
[40] Maa MC, Leu TH, McCarley DJ, Schatzman RC and Parsons SJ. Potentiation of epidermal growth factor receptor-mediated oncogenesis by c-Src: implications for the etiology of multiple human cancers. Proc Natl Acad Sci U S A 1995; 92: 6981-6985.
[41] Murakami Y, Sonoda K, Abe H, Watari K, Kusakabe D, Azuma K, Kawahara A, Akiba J, Oneyama C, Pachter JA, Sakai K, Nishio K, Kuwano M and Ono M. The activation of SRC family kinases and focal adhesion kinase with the loss of the amplified, mutated EGFR gene contributes to the resistance to afatinib, erlotinib and osimertinib in human lung cancer cells. Oncotarget 2017; 8: 70736-70751.
[42] Gold KA, Lee JJ, Harun N, Tang X, Price J, Kawedia JD, Tran HT, Erasmus JJ, Blumenschein GR, William WN, Wistuba II and Johnson FM. A phase I/II study combining erlotinib and dasatinib for non-small cell lung cancer. Oncologist 2014; 19: 1040-1041.
[43] Creelan BC, Gray JE, Tanvetyanon T, Chiappori AA, Yoshida T, Schell MJ, Antonia SJ and Haura EB. Phase 1 trial of dasatinib combined with afatinib for epidermal growth factor receptor-(EGFR-) mutated lung cancer with acquired tyrosine kinase inhibitor (TKI) resistance. Br J Cancer 2019; 120: 791-796.
[44] Johnson ML, Riely GJ, Rizvi NA, Azzoli CG, Kris MG, Sima CS, Ginsberg MS, Pao W and Miller VA. Phase II trial of dasatinib for patients with acquired resistance to treatment with the epidermal growth factor receptor tyrosine kinase inhibitors erlotinib or gefitinib. J Thorac Oncol 2011; 6: 1128-1131.
[45] Fruman DA, Chiu H, Hopkins BD, Bagrodia S, Cantley LC and Abraham RT. The PI3K pathway in human disease. Cell 2017; 170: 605-635.
[46] Webb DJ, Donais K, Whitmore LA, Thomas SM, Turner CE, Parsons JT and Horwitz AF. FAK-Src signalling through paxillin, ERK and MLCK regulates adhesion disassembly. Nat Cell Biol 2004; 6: 154-161.
[47] Bubici C and Papa S. JNK signalling in cancer: in need of new, smarter therapeutic targets. Br J Pharmacol 2014; 171: 24-37.
[48] Xie G, Peng Z and Raufman JP. Src-mediated aryl hydrocarbon and epidermal growth factor receptor cross talk stimulates colon cancer cell proliferation. Am J Physiol Gastrointest Liver Physiol 2012; 302: G1006-1015.
[49] Laham-Karam N, Pinto GP, Poso A and Kokkonen P. Transcription and translation inhibitors in cancer treatment. Front Chem 2020; 8: 276.
[50] Piu F, Gauthier NK, Olsson R, Currier EA, Lund BW, Croston GE, Hacksell U and Brann MR. Identification of novel subtype selective RAR agonists. Biochem Pharmacol 2005; 71: 156-162.
[51] Zhang Y, Au Q, Zhang M, Barber JR, Ng SC and Zhang B. Identification of a small molecule SIRT2 inhibitor with selective tumor cytotoxicity. Biochem Biophys Res Commun 2009; 386: 729-733.
[52] Karwaciak I, Gorzkiewicz M, Ryba K, Dastych J, Pulaski L and Ratajewski M. AC-93253 triggers the downregulation of melanoma progression

markers and the inhibition of melanoma cell proliferation. Chem Biol Interact 2015; 236: 9-18.
[53] Reddy AS and Zhang S. Polypharmacology: drug discovery for the future. Expert Rev Clin Pharmacol 2013; 6: 41-47.
[54] Ramsay RR, Popovic-Nikolic MR, Nikolic K, Uliassi E and Bolognesi ML. A perspective on multi-target drug discovery and design for complex diseases. Clin Transl Med 2018; 7: 3.
[55] Rutkowski P, Jagielska B, Andrzejuk J, Bylina E, Lugowska I, Switaj T, Kosela-Paterczyk H, Kozak K, Falkowski S and Klimczak A. The analysis of the long-term outcomes of sorafenib therapy in routine practice in imatinib and sunitinib resistant gastrointestinal stromal tumors (GIST). Contemp Oncol (Pozn) 2017; 21: 285-289.
[56] Han B, Li K, Zhao Y, Li B, Cheng Y, Zhou J, Lu Y, Shi Y, Wang Z, Jiang L, Luo Y, Zhang Y, Huang C, Li Q and Wu G. Anlotinib as a third-line therapy in patients with refractory advanced non-small-cell lung cancer: a multicentre, randomised phase II trial (ALTER0302). Br J Cancer 2018; 118: 654-661.

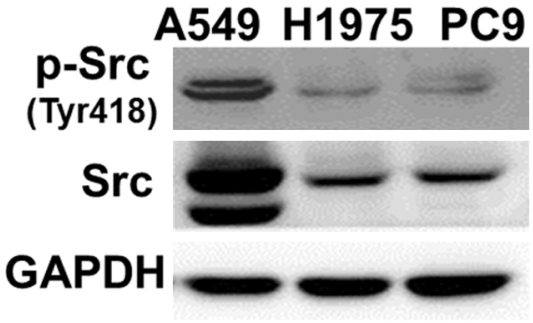

Figure S1. The expression and phosphorylation of Src in different non-small cell lung cancer cell lines. An immunoblot analysis was performed to measure Src levels in the A549, H3255 and H1975 cell lines. The results show that the Src phosphorylation and protein expression were higher in A549 cells than those in the other two cell lines. GAPDH was used as an internal control. Each experiment was performed independently and in triplicate.

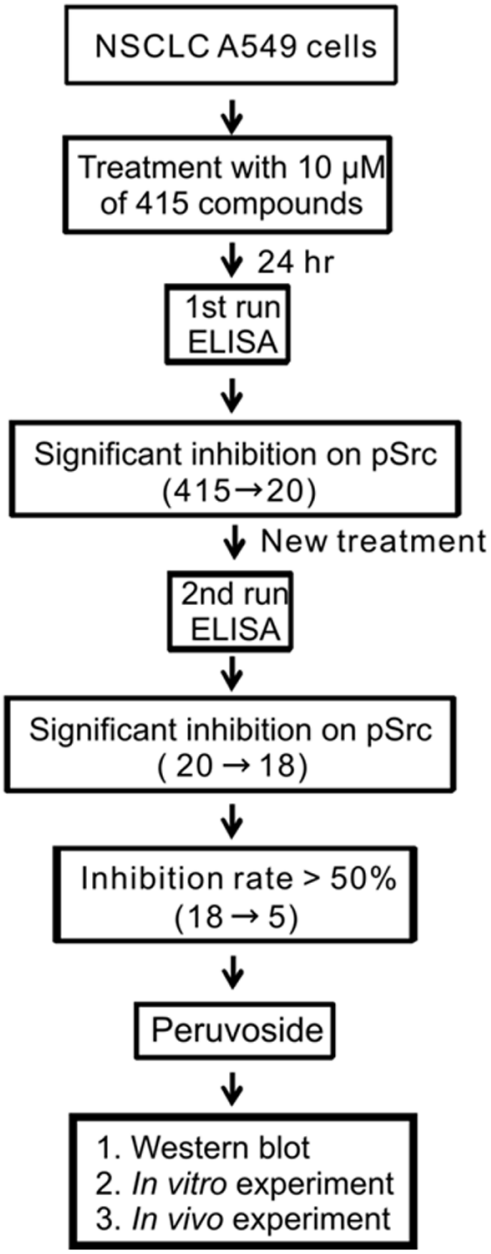

Figure S2. Criteria and procedures for drug screening. The designated criteria and procedures were employed to identify candidate compounds that could suppress pSrc activity and repress cancer cell function *in vitro* and *in vivo*.

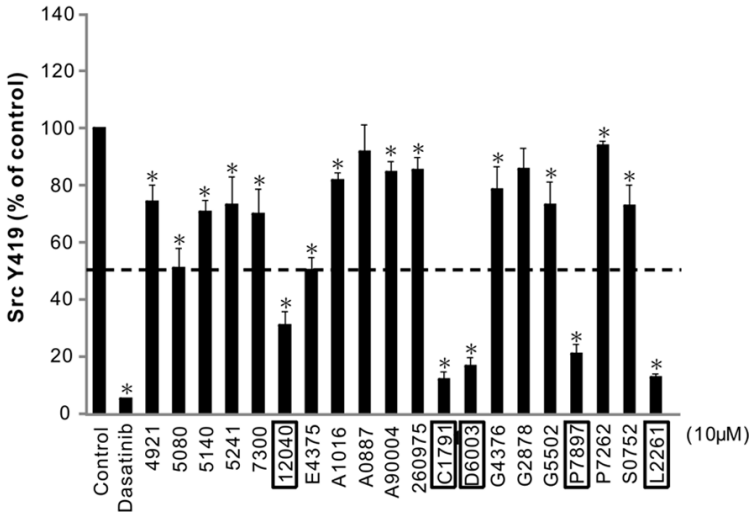

Figure S3. Effects of the candidate compounds on Src Y419 in the A549 NSCLC cell line. Src phosphorylation in A549 cells treated with the candidate compounds for 24 h was determined by an ELISA. Dasatinib was used as a positive control. The results are presented as percentages of the vehicle control (0.1% DMSO). Each experiment was performed independently and in triplicate. *P < 0.05 compared with the vehicle control. P7897 (peruvoside) is the main drug used in this study.

Table S1. The IC_{50} values of A549, PC9, PC9/gef, H3255, H1975 and BEAS-2B with peruvoside treatment for various times

Time	Peruvoside IC_{50} (μM)					
	A549	PC9	PC9/gef	H3255	H1975	BEAS2B
24 hr	0.048 ± 0.004	0.074 ± 0.005	0.067 ± 0.006	0.143 ± 0.012	0.277 ± 0.037	0.428 ± 0.041
48 hr	0.011 ± 0.001	0.038 ± 0.004	0.035 ± 0.004	0.041 ± 0.004	0.230 ± 0.019	0.037 ± 0.002
72 hr	0.006 ± 0.003	0.033 ± 0.026	0.031 ± 0.002	0.035 ± 0.004	0.056 ± 0.004	0.022 ± 0.002
96 hr	0.005 ± 0.003	0.031 ± 0.002	0.030 ± 0.001	0.031 ± 0.002	0.031 ± 0.003	0.025 ± 0.003

Table S2. The combination index (CI) and fractional effect (FE) of combination treatment with peruvoside and gefitinib (Iressa) in lung cancer A549 cells

Gefitinib (μM)	Peruvoside					
	0.005		0.0075		0.01	
	FE	CI	FE	CI	FE	CI
0.01	0.257 ± 0.103	0.700 ± 0.511	0.751 ± 0.224	0.420 ± 0.494	0.914 ± 0.027	0.200 ± 0.200
0.05	0.530 ± 0.384	0.275 ± 0.269	0.890 ± 0.154	0.219 ± 0.308	0.793 ± 0.04	0.448 ± 0.448
0.1	0.677 ± 0.254	0.121 ± 0.054	0.650 ± 0.079	0.555 ± 0.048	0.757 ± 0.014	0.549 ± 0.549
0.25	0.419 ± 0.092	0.304 ± 0.005	0.377 ± 0.036	0.414 ± 0.081	0.999 ± 0.001	0.012 ± 0.012
0.5	0.306 ± 0.017	0.768 ± 0.312	0.433 ± 0.003	0.383 ± 0.118	0.925 ± 0.059	0.311 ± 0.311

Table S3. The CI and FE of combination treatment with peruvoside and gefitinib (Iressa) in lung cancer PC9/gef cells

Gefitinib (μM)	Peruvoside					
	0.01		0.025		0.05	
	FE	CI	FE	CI	FE	CI
0.01	0.286 ± 0.186	1.271 ± 0.192	0.416 ± 0.053	0.838 ± 0.226	0.956 ± 0.042	0.229 ± 0.018
0.05	0.298 ± 0.157	1.133 ± 0.330	0.536 ± 0.071	0.793 ± 0.263	0.971 ± 0.029	0.169 ± 0.011
0.1	0.306 ± 0.211	1.054 ± 0.299	0.717 ± 0.036	0.589 ± 0.141	0.918 ± 0.025	0.255 ± 0.069
0.25	0.328 ± 0.171	1.007 ± 0.452	0.557 ± 0.005	0.733 ± 0.074	0.902 ± 0.023	0.330 ± 0.122
0.5	0.360 ± 0.148	0.915 ± 0.314	0.631 ± 0.027	0.417 ± 0.177	0.935 ± 0.046	0.150 ± 0.107

Table S4. The CI and FE of combination treatment with peruvoside and gefitinib (Iressa) in lung cancer H1975 cells

Gefitinib (μM)	Peruvoside					
	0.01		0.025		0.05	
	FE	CI	FE	CI	FE	CI
0.01	0.022 ± 0.020	2.951 ± 0.018	0.511 ± 0.016	0.628 ± 0.018	0.882 ± 0.013	0.435 ± 0.270
0.05	0.176 ± 0.008	1.806 ± 0.042	0.624 ± 0.010	0.528 ± 0.010	0.716 ± 0.034	0.399 ± 0.296
0.1	0.085 ± 0.000	2.335 ± 1.287	0.755 ± 0.032	0.423 ± 0.026	0.918 ± 0.062	0.399 ± 0.318
0.25	0.085 ± 0.008	2.004 ± 0.127	0.601 ± 0.010	0.353 ± 0.031	0.853 ± 0.008	0.512 ± 0.243
0.5	0.250 ± 0.02	1.425 ± 0.243	0.701 ± 0.019	0.453 ± 0.066	0.869 ± 0.030	0.531 ± 0.259

Table S5. Basic information of the 18 chemicals that showed a significant inhibitory effect compared with that of the control

Code	Name	CASN	Chemical Family	Chemical Formula
5080	EMBELIN (RG)	550-24-3	Quinones	C17H26O4
5140	EPIESTRIOL, 16-(RG)	547-81-9	Steroids	C18H24O3
5241	ESCULETIN (P)	305-01-1	Coumarins	C9H6O4
7300	GLUCOTROPAEOLIN POTASSIUM SALT (SH)	5115-71-9	Glucosinolates	C14H18KNO9S2
12040	LANATOSIDE B (RG)	17575-21-2	Cardiac glycosides	C49H76O20
E4375	ADRENALINE, L-(RG)	51-43-4	Alkaloids	C9H13NO3
A1016	AMARANTH (RG)	915-67-3	Dyes	C20H11N2Na3O10S3
A90004	ANTHRAQUINONE (RG)	84-65-1	Quinones	C14H8O2
260975	BROMOCINNAMIC ACID, 4-(RG)	50663-21-3	Phenolic acids	C9H7BrO2
C1791	CRESYL ACETATE, m-(P)	122-46-3	Phenolic acids	C9H10O2
D6003	DIGOXIN (RG)	20830-75-5	Cardiac glycosides	C41H64O14
G4376	GLUTATHIONE (OXIDIZED) (RG)	27025-41-8	Tripeptide	C20H32N6O12S2
G5502	GUAIACOL (P)	90-05-1	Phenolic acids	C7H8O2
P7897	PERUVOSIDE (RG)	1182-87-2	Cardiac glycosides	C30H44O9
P7262	PLUMBAGIN (RG)	481-42-5	Quinones	C11H8O3
S0752	SYNEPHRINE (P)	94-07-5	Alkaloids	C9H13NO2
L2261	LANATOSIDE C	17575-22-3	Cardiac glycosides	C49H76O20

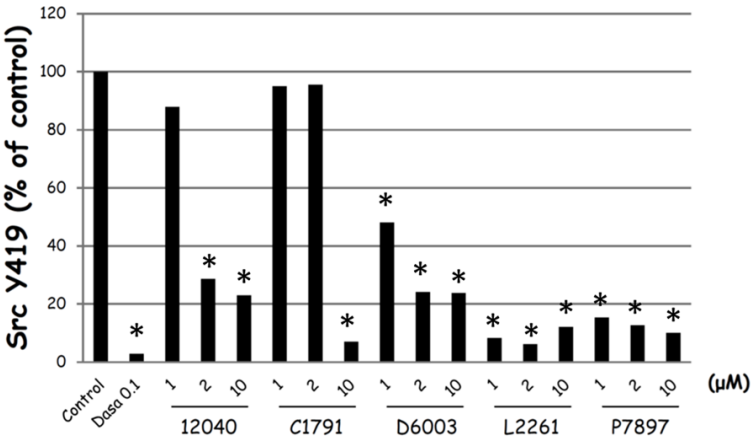

Figure S4. Effects of the top 5 candidate compounds on Src Y419 in the A549 NSCLC cell line. Src phosphorylation in A549 cells treated with low concentrations of the top 5 candidate compounds for 24 h was determined by an ELISA. Dasa 0.1 was used as a positive control. The results are presented as percentages of the vehicle control (0.1% DMSO). Each experiment was performed independently and in triplicate. *P<0.05 compared with the vehicle control. P7897 (peruvoside) is the main drug used in this study.

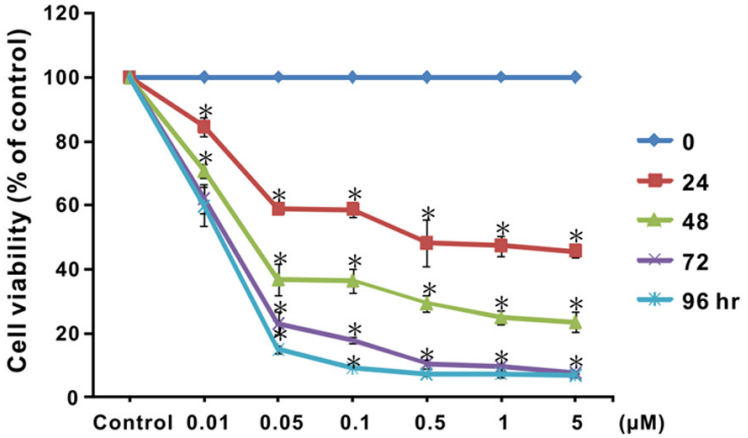

Figure S5. Cytotoxic effects of peruvoside on non-tumour BEAS2B cells, as determined by cell viability assay. PrestoBlue cell viability assay was performed to investigate the cytotoxic effects of peruvoside after treatment. The IC_{50} values at 24, 48, 72 and 96 hours were 0.428, 0.037, 0.022 and 0.025 μM, respectively. Each experiment was performed independently and in triplicate. *P < 0.05 compared with control (0.1% DMSO).